ACS APPLIED MATERIALS & INTERFACES

RESEARCH ARTICLE

www.acsami.org

CdS/CdSe-Cosensitized TiO_2 Photoanode for Quantum-Dot-Sensitized Solar Cells by a Microwave-Assisted Chemical Bath Deposition Method

Guang Zhu, Likun Pan,* Tao Xu, and Zhuo Sun

Engineering Research Center for Nanophotonics & Advanced Instrument, Ministry of Education, Department of Physics, East China Normal University, Shanghai 200062, China

ABSTRACT: A CdS/CdSe quantum-dot (QD)-cosensitized TiO_2 film has been fabricated using a microwave-assisted chemical bath deposition technique and used as a photoanode for QD-sensitized solar cells. The technique allows a direct and rapid deposition of QDs and forms a good contact between QDs and TiO_2 films. The photovoltaic performance of the as-prepared cell is investigated. The results show that the performance of the CdS/CdSe-cosensitized cell achieves a short-circuit current density of 16.1 mA cm^{-2} and a power conversion efficiency of 3.06% at one sun (AM 1.5 G, 100 mW cm^{-2}), which is comparable to the one fabricated using conventional successive ionic layer adsorption and reaction technique.

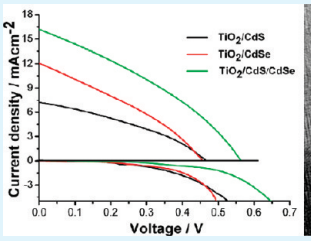

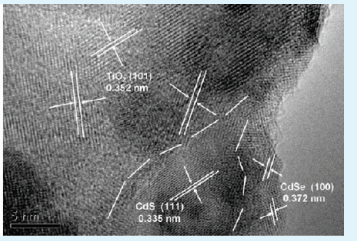

KEYWORDS: solar cells, quantum dots, electrodes, microwave-assisted chemical bath deposition, titanium dioxide

INTRODUCTION

Dye-sensitized solar cells have attracted considerable attention and represent a key class of cell architecture that has emerged as a promising candidate for the development of next-generation solar cells.[1−9] Pursuing high efficiency is always a core task for solar cells, and one of the current key issues is to search the suitable panchromatic sensitizers for enhancing the light harvest in a visible-light region. In recent years, quantum dots (QDs) have been employed as sensitizers because of their high extinction coefficient, spectral tunability by particle size, and good stability.[10−37] Among the semiconductor QDs, CdS and CdSe have been paid much more attention because of their high potential in the light harvest in a visible-light region.[7,29] Compared with single (CdS and CdSe) QDs, their cosensitized structure can provide a superior ability owing to extension of the light absorption range and effective charge injection from QDs to TiO_2.[7−9] Attempts to combine CdS and CdSe QDs to assemble on TiO_2 nanoparticles, nanowires, or nanotubes have been reported in efforts to obtain efficient QD-sensitized solar cells (QDSSCs) with power conversion efficiencies of 2−3%.[7−9,38−47] It should be noticed that, to date, these QDSSCs based on a cosensitized porous TiO_2 electrode have been almost fabricated by a successive ionic layer adsorption and reaction (SILAR) method, which requires the repetitive immersing operation of a TiO_2 film in precursor solutions containing Cd, S, or Se.

As an inexpensive, quick, clean, versatile technique, microwave irradiation induces interaction of the dipole moment of polar molecules in a solvent with alternating electronic and magnetic fields, causing molecular-level heating, which leads to homogeneous and quick thermal reactions.[48,49] If such a heating is performed in closed vessels under high pressure, more energy input at the same temperature and enormous accelerations in the reaction time can be achieved, which means that a reaction in the conventional solvothermal method that takes several hours can be completed over the course of minutes or a reaction that would not proceed previously will now proceed, typically with higher yields.[50] However, the microwave technique has seldom been studied up until now to deposit CdS/CdSe QDs onto a TiO_2 electrode for QDSSCs, although such a method has been used successfully to fabricate CdS, CdSe, and CdSe/CdS QDs, respectively.[51−53]

In our recent works, we have fabricated CdS and CdSe QDSSCs using a simple, rapid, and effective microwave-assisted chemical bath deposition (MACBD) method.[54,55] This method can synthesize rapidly CdS or CdSe QDs and form a good contact between QDs and the TiO_2 layer. Importantly, MACBD avoids the repetitive immersing operation, organic linker, or high-temperature heating required in other conventional methods, while the cells fabricated using MACBD exhibit photovoltaic performances comparable to those using other methods. In this work, we further explore application of the MACBD method in the fabrication of a CdS/CdSe-cosensitized TiO_2 photoanode for QDSSCs. The as-synthesized CdS/CdSe QDSSCs show a high short-circuit current density of 16.1 mA cm^{-2} and a conversion efficiency of 3.06% under one sun illumination compared with the cell fabricated using the SILAR method.

Received: May 21, 2011
Accepted: July 11, 2011
Published: July 11, 2011

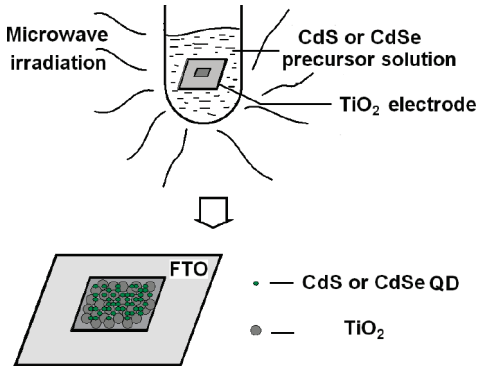

Figure 1. Schematic diagram of the MACBD process.

EXPERIMENTAL SECTION

A TiO_2 electrode was prepared by the screen printing of TiO_2 paste onto the F-doped SnO_2 (FTO; resistivity 14 $\Omega\ \square^{-1}$; Nippon Sheet Glass, Tokyo, Japan) glass.[56] The electrode configuration was a transparent layer of nanocrystalline TiO_2 (P25, Degussa) with a mean size of 25 nm and a scattering layer microcrystalline TiO_2 (Dalian HeptaChroma SolarTech Co., Ltd.) with a mean size of 200 nm. Such a double-layer structure favors contact between the substrate and electrode and enhances the light scattering ability, which can improve the performance of the cells.[57] The as-prepared electrodes were sintered at 500 °C for 30 min.

The as-prepared TiO_2 electrodes were sensitized by CdS and CdSe QDs by the MACBD process,[54,55] as shown in Figure 1. For CdS deposition, the electrodes were immersed in a sealed vessel with a CdS precursor aqueous solution [0.05 M $Cd(NO_3)_2$ and 0.05 M CH_4N_2S, Sinopharm Chemical Reagents Co. Ltd.], and then the vessel was put into an automated focused microwave system (Explorer-48, CEM Co.) and treated at 150 °C with a microwave irradiation power of 100 W for 30 min. For subsequent CdSe deposition, Se powder (32 mg) was added in a mixture of 10 mL of 0.04 M $Cd(NO_3)_2$ and 10 mL of 0.04 M Na_2SO_3 (Sinopharm Chemical Reagents Co. Ltd.) as a precursor aqueous solution. The CdS-deposited TiO_2 electrodes were immersed in a CdSe precursor aqueous solution and then treated at 150 °C with a microwave irradiation power of 100 W for 20 min. In experiments, the effect of the synthesis conditions on the device performance has been carefully studied and their selection is based on our previous works.[54,55] In this work, in order to compare the performances of QDSSCs using different methods, CdS/CdSe was also deposited on the TiO_2 film by the SILAR method. The detailed information can be found elsewhere.[5,7]

The morphology and structures of TiO_2, TiO_2/CdS, and TiO_2/CdS/CdSe electrodes were characterized using a Hitachi S-4800 field emission scanning electron microscope and a JEOL-2010 high-resolution transmission electron microscope, respectively. The UV−vis absorption spectra of electrodes were detected using a UV−vis spectrophotometer (Hitachi U-3900).

The CdS/CdSe-cosensitized QDSSCs were sealed in a sandwich structure with a 25 μm spacer (Surlyn) by using thin Au-sputtered FTO glass as the counter electrode. A water/methanol (3:7 by volume) solution was used as a cosolvent of the polysulfide electrolyte.[58] The electrolyte solution consists of 0.5 M Na_2S, 2 M S, and 0.2 M KCl. It should be noticed that methanol as a sacrificial agent can provide a sacrificial donor in the system by scavenging photogenerated holes.[59,60] Although the contribution of the conversion efficiency from methanol should be small because of the existence of a large number of S^{2-}/S_n^{2-} redox couples to scavenge and transfer most of holes, further optimization of the electrolyte to get rid of the alcohol in it should be concerns in future work. The active area of the cell is 0.2 cm^2. $J-V$ measurement was performed with a Keithley model 2440 sourcemeter and a Newport solar simulator system (equipped with a 1 kW xenon arc lamp, Oriel) at one sun (AM 1.5 G, 100 mW cm^{-2}). The incident photon-to-current conversion efficiency (IPCE) was measured as a function of the wavelength from 300 to 800 nm using an Oriel 300W xenon arc lamp and a lock-in amplifier M 70104 (Oriel) under monochromator illumination.

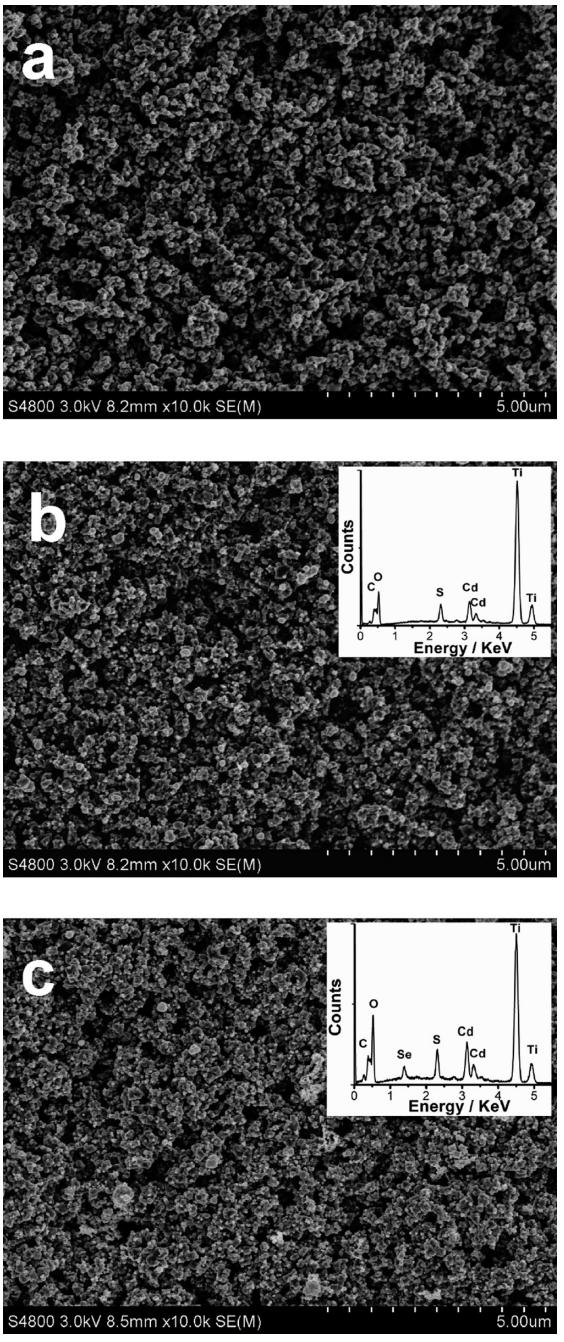

Figure 2. Surface morphologies of (a) a pure TiO_2 electrode, (b) the TiO_2/CdS electrode, and (c) the TiO_2/CdS/CdSe electrode by FESEM measurement. The insets in parts b and c show the EDS spectra.

RESULTS AND DISCUSSION

Figure 2a shows the field emission scanning electron microscopy (FESEM) images (top view) of pure TiO_2 films. The TiO_2

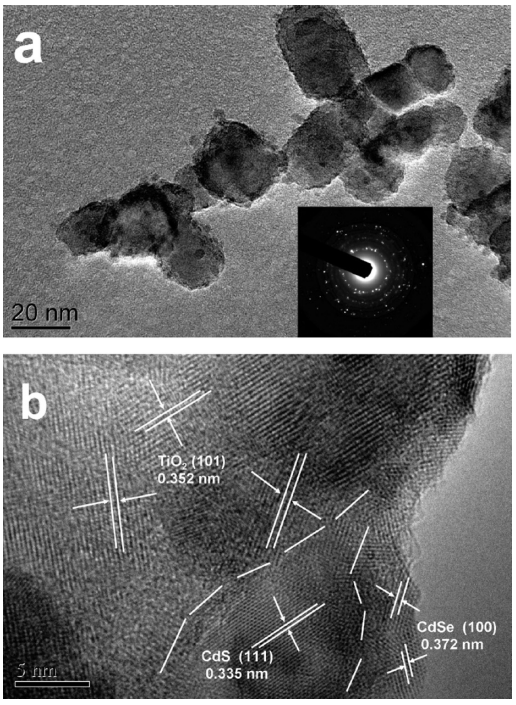

Figure 3. (a) Low- and (b) high-magnification HRTEM images of the TiO_2/CdS/CdSe electrode. The inset in part a shows the corresponding SAED pattern.

electrode is constructed by a random agglomeration of TiO_2 particles. The porous structure of TiO_2 favors an easy penetration of the electrolyte, as well as Cd, S, and Se precursors, during deposition. Figure 2b shows the FESEM image (top view) of the TiO_2/CdS electrode obtained by MACBD. Compared with a pure TiO_2 electrode (Figure 2a), an amount of CdS nanoparticles is observed to deposit on the surface of the TiO_2 film. The composition of the electrode was identified by energy-dispersive X-ray spectroscopy (EDS) measurement, as shown in the inset of Figure 2b. Quantitative analysis of the EDS spectrum gives a Cd: S atomic ratio of about 1, indicating that high-grade CdS particles are formed. A more compact surface layer for the TiO_2/CdS/CdSe electrode is clearly observed in Figure 2c compared with Figure 2b, which indicates that an amount of CdSe QDs is assembled on the surface of the TiO_2/CdS electrode by MACBD. The Cd, Se, and S peaks are clearly observed in the EDS spectrum of the electrode, as shown in the inset of Figure 2c. Quantitative analysis of the EDS spectrum reveals that the atomic ratio of Cd versus S plus Se is nearly 1, indicating that the deposited CdS and CdSe QDs are likely to be stoichiometric. The result confirms that CdS and CdSe QDs are successfully assembled on the surface of the TiO_2 film via the MACBD process.

Figure 3a shows a low-magnification high-resolution transmission electron microscopy (HRTEM) image of the TiO_2/CdS/CdSe electrode. It is clearly found that the surface of the TiO_2 particles is decorated with QDs (black dots). The corresponding selected-area electron diffraction (SAED) pattern in the inset of Figure 3a indicates that the electrode is a polycrystalline structure. Figure 3b shows a high-magnification HRTEM image of the TiO_2/CdS/CdSe electrode. The lattice spacing measured for the crystalline plane is 0.352 nm, corresponding to the (101) plane of TiO_2 (JCPDS 21-1272). Around the TiO_2 crystallite,

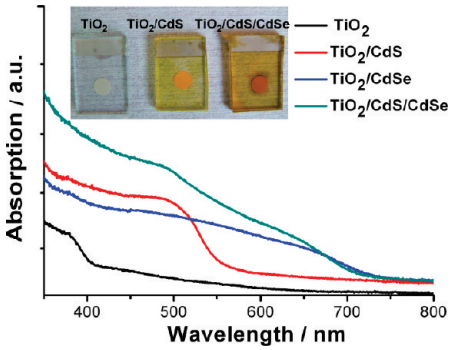

Figure 4. UV−vis absorption spectra of the TiO_2, TiO_2/CdS, TiO_2/CdSe, and TiO_2/CdS/CdSe electrodes. The insets are the photographs of the TiO_2, TiO_2/CdS, and TiO_2/CdS/CdSe electrodes.

fine crystallites with various orientations and lattice spacing are observed. By careful measurement and comparison of the lattice parameters with the data in JCPD, the crystallites connecting to TiO_2 have a lattice fringe of 0.335 nm, which is ascribed to the (111) plane of CdS (JCPDS 80-0019), and outer layer crystallites with lattice spacing of 0.372 nm, next to the CdS layer, correspond to the (100) plane of CdSe (JCPDS 77-2307). These results further prove that CdS and CdSe nanocrystals have been successfully deposited on the surface of porous TiO_2 to finally form a TiO_2/CdS/CdSe cascade structure.

Figure 4 shows the UV−vis absorption spectra of pure TiO_2, TiO_2/CdS, TiO_2/CdSe, and TiO_2/CdS/CdSe electrodes. The inset of Figure 4 shows the photoimages for pure TiO_2, TiO_2/CdS, and TiO_2/CdS/CdSe electrodes. After CdSe QDs are deposited, the color of the electrode changes from yellow to orange. Compared with the absorption spectra of the pure TiO_2 film, there are obvious absorption peaks near 500 and 650 nm for the TiO_2/CdS and TiO_2/CdSe electrodes. The band gaps (absorption edges) of CdS and CdSe QDs are about 2.30 and 1.80 eV, which are extracted from the absorption spectra using the Tauc plot method[61,62] and are higher than the values of bulk CdS and CdSe due to the quantum size effect.[63] In the meantime, it can be seen that the optical range of TiO_2/CdS/CdSe is broader than those of TiO_2/CdS and TiO_2/CdSe. Therefore, the cosensitization effect of CdS and CdSe QDs can be observed by extension of the absorption range and the increase of absorbance.[9,39]

The IPCE curves of QDSSCs with the TiO_2/CdS, TiO_2/CdSe, and TiO_2/CdS/CdSe electrodes, as shown in Figure 5, exhibit trends similar to those of the UV−vis spectra. CdS- and CdSe-sensitized cells demonstrate IPCE peak values of 65% and 40%, respectively. However, the IPCE peak value reaches 73% for the CdS/CdSe-cosensitized cell, which is ascribed to the joint contributions from CdS and CdSe QDs in the light harvest.

The $J-V$ curves of QDSSCs with the TiO_2/CdS, TiO_2/CdSe, and TiO_2/CdS/CdSe electrodes at one sun (AM 1.5 G, 100 mW cm^{-2}) and in dark conditions are shown in Figure 6. The short-circuit current density (J_{sc}), open-circuit potential (V_{oc}), fill factor (FF), and conversion efficiency (η) of CdS- and CdSe-sensitized cells are 7.20 mA cm^{-2}, 0.46 V, 0.35, and 1.18% and 12.1 mA cm^{-2}, 0.45 V, 0.32, and 1.75%, respectively. The higher efficiency of CdSe-sensitized QDSSCs is attributed to its broader light absorption range than that of CdS, and the lower FF of CdSe-sensitized QDSSCs should be due to a low driving force for electron injection.[7,9,40] When both QDs are combined

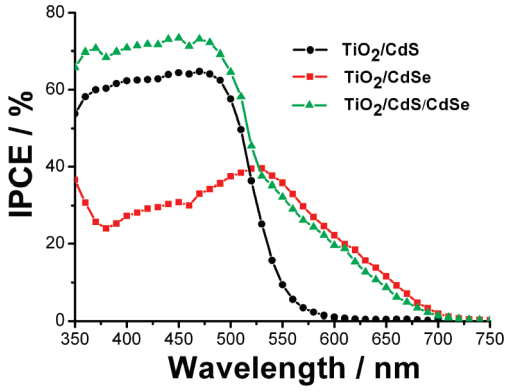

Figure 5. IPCE curves of QDSSCs with the TiO_2/CdS, TiO_2/CdSe, and TiO_2/CdS/CdSe electrodes.

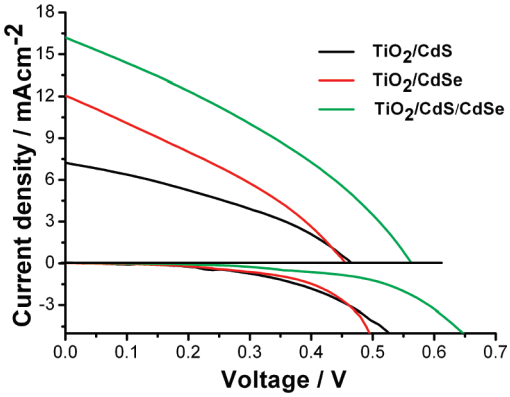

Figure 6. $J-V$ curves of QDSSCs with the TiO_2/CdS, TiO_2/CdSe, and TiO_2/CdS/CdSe electrodes under one sun illumination (AM 1.5 G, 100 mW cm^{-2}) and in dark conditions.

sequentially in a cosensitized structure, synergistic improvement in J_{sc} (16.1 mA cm^{-2}) and V_{oc} (0.56 V) is observed with a slight change in FF (0.34), leading to a high conversion efficiency of 3.06%. The higher V_{oc} may be due to efficient QD coverage on the TiO_2 film[8] and reduction of recombination loss at interfaces.[64] In addition to the enhanced visible-light absorption, the large increase in J_{sc} and η for CdS/CdSe-cosensitized QDSSCs is ascribed to the following reasons:[8,9,40,44] (1) the cascade energy level structure (Figure 7) in the order of TiO_2 < CdS < CdSe is formed via the combination of CdS and CdSe, as reported by others.[5,7,38] The favorable alignment of the Fermi levels at TiO_2/CdS/CdSe interfaces facilitates electron injection and hole recovery for both inner CdS and outer CdSe layers; (2) the CdS underlayer promotes the growth of the CdSe layer due to less mismatched constants and more similar chemistries between them[8,46] and more QD loading might enhance the photocurrent density. The latter effect is confirmed by the absorption spectra presented in Figure 4. The smaller dark current for CdS/CdSe QDSSCs observed from the $J-V$ curves of the cells in dark conditions indicates that CdS/CdSe QDSSCs have a superior interfacial structure to inhibit the interfacial recombination of the injected electrons from TiO_2 to the electrolyte,[5,7,38,54] which is also responsible for its higher conversion efficiency.

The stability test of CdS/CdSe QDSSCs was carried out at different time intervals, and the results are shown in Figure 8. It is

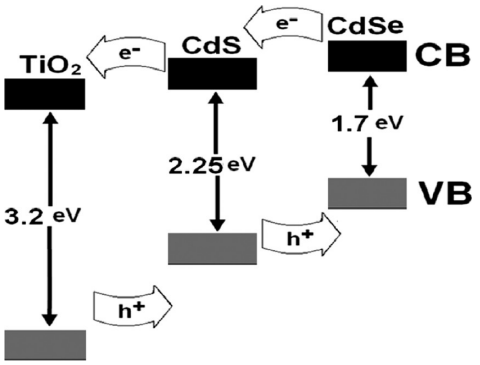

Figure 7. Energy-band structures of TiO_2, CdS, and CdSe in bulk. CB = conduction band; VB = valence band.

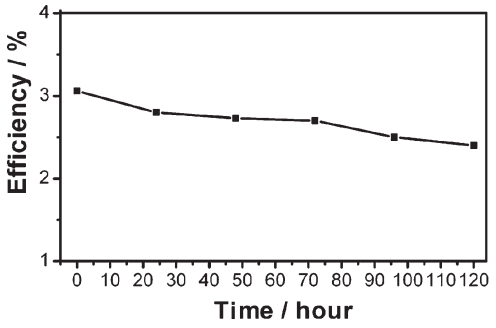

Figure 8. Variation of the conversion efficiency of QDSSCs with the TiO_2/CdS/CdSe electrode as a function of time.

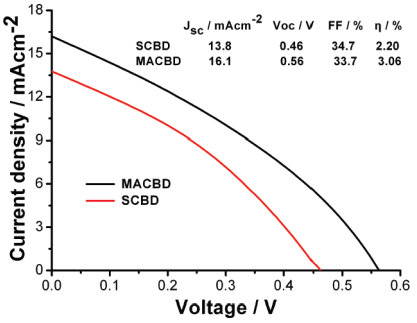

Figure 9. $J-V$ curves of QDSSCs with TiO_2/CdS/CdSe electrodes by MACBD and SILAR techniques under one sun illumination (AM 1.5 G, 100 mW cm^{-2}).

found that about 20% degradation of η is observed after 100 h mainly because of photoanodic corrosion.[65] Several studies have introduced a wide-band-gap semiconductor (typically ZnS) passivation layer onto the surface of the QD sensitizer to suppress photoanodic corrosion and improve the cell efficiency and stability.[65−67] Therefore, further improvement in the cell performance can be expected by introducing and optimizing the passivation layer in future work.

Figure 9 displays $J-V$ curves of QDSSCs based on TiO_2/CdS/CdSe electrodes fabricated by MACBD and SILAR (for comparison) techniques, respectively. It can be observed that higher performances of CdS/CdSe QDSSCs are achieved via MACBD compared with the conventional SILAR technique.

The higher η for the cell using the MACBD technique should be ascribed to the following reasons: (i) Good contact between QDs and the TiO_2 layer is formed as a result of rapidly elevated temperature during microwave irradiation. QD deposition on the surface of TiO_2 via the MACBD method is a three-step process.[54] The CdS or CdSe nuclei grow, crystallize, and stabilize on TiO_2 under microwave irradiation,[68] leading to a good contact between QDs and TiO_2. On the other hand, microwave irradiation has been used to prepare the hydrophilic nanoparticles[69] or to improve the surface wettability of the polymer by increasing the surface free energy.[54,55,70] Such a superior interface between TiO_2 and QDs via the MACBD method can inhibit the interfacial recombination of the injected electrons from TiO_2 to the electrolyte, which is responsible for its higher η.[71] (ii) Microwave irradiation can heat up the aqueous solution homogeneously and quickly because of the penetration characteristics of microwaves and the high utilization factor of the microwave energy.[72,73] Therefore, the nucleation and growth of CdS and CdSe QDs can be finished in an extremely short period of time, which is extraordinarily beneficial for reducing the concentration of surface defects of QDs.[74,75] The carrier recombination at surface defects of QDs is correspondingly suppressed, and thus the cell performance is increased.[76,77]

CONCLUSIONS

In summary, a CdS/CdSe-cosensitized TiO_2 film as a photoanode for QDSSCs has been prepared by using a simple, rapid, and effective MACBD technique. This technique can synthesize CdS and CdSe QDs rapidly and suppress their surface defects as well as form a good contact between QDs and the TiO_2 film. A short-circuit current density of 16.1 mA cm^{-2} and a conversion efficiency of 3.06% under one sun illumination has been achieved by using the MACBD method, which is comparable to those by using a conventional SILAR method. However, MACBD avoids the repetitive immersing operation required in SILAR. The present synthetic strategy should be a promising fabrication technique for highly efficient QDSSCs.

AUTHOR INFORMATION

Corresponding Author

*Tel: 86 21 62234132. Fax: 86 21 62234321. E-mail: lkpan@phy.ecnu.edu.cn.

ACKNOWLEDGMENT

This work was supported by Special Project for Nanotechnology of Shanghai (Grant 1052 nm02700).

REFERENCES

(1) O'Regan, B.; Grätzel, M. *Nature* **1991**, *353*, 737–740.
(2) Grätzel, M. *Nature* **2001**, *414*, 338–344.
(3) Kamat, P. V.; Tvrdy, K.; Baker, D. R.; Radich, J. G. *Chem. Rev.* **2010**, *110*, 6664–6688.
(4) Muduli, S.; Lee, W.; Dhas, V.; Mujawar, S.; Dubey, M.; Vijayamohanan, K.; Han, S. H.; Ogale, S. *ACS Appl. Mater. Interfaces* **2009**, *1*, 2030–2035.
(5) Lee, Y. L.; Chi, C. F.; Liau, S. Y. *Chem. Mater.* **2010**, *22*, 922–927.
(6) Joshi, P.; Zhang, L. F.; Chen, Q. L.; Galipeau, D.; Fong, H.; Qiao, Q. Q. *ACS Appl. Mater. Interfaces* **2010**, *2*, 3572–3577.
(7) Lee, Y. L.; Lo, Y. S. *Adv. Funct. Mater.* **2009**, *19*, 604–609.
(8) Sudhagar, P.; Jung, J. H.; Park, S.; Lee, Y. G.; Sathyamoorthy, R.; Kang, Y. S.; Ahn, H. *Electrochem. Commun.* **2009**, *11*, 2220–2224.
(9) Chen, J.; Zhao, D. W.; Song, J. L.; Sun, X. W.; Deng, W. Q.; Liu, X. W.; Lei, W. *Electrochem. Commun.* **2009**, *11*, 2265–2267.
(10) Hwang, J. Y.; Lee, S. A.; Lee, Y. H.; Seok, S. I. *ACS Appl. Mater. Interfaces* **2010**, *2*, 1343–1348.
(11) Xie, Y.; Ali, G.; Yoo, S. H.; Cho, S. O. *ACS Appl. Mater. Interfaces* **2010**, *2*, 2910–2914.
(12) Gao, X. F.; Li, H. B.; Sun, W. T.; Chen, Q.; Tang, F. Q.; Peng, L. M. *J. Phys. Chem. C* **2009**, *113*, 7531–7535.
(13) Lee, Y. H.; Im, S. H.; Rhee, J. H.; Lee, J. H.; Seok, S. I. *ACS Appl. Mater. Interfaces* **2010**, *2*, 1648–1652.
(14) Gao, X. F.; Sun, W. T.; Hu, Z. D.; Ai, G.; Zhang, Y. L.; Feng, S.; Li, F.; Peng, L. M. *J. Phys. Chem. C* **2009**, *113*, 20481–20485.
(15) Shalom, M.; Ruhle, S.; Hod, I.; Yahav, S.; Zaban, A. *J. Am. Chem. Soc.* **2009**, *131*, 9876–9877.
(16) Zhu, G.; Cheng, Z. J.; Lv, T.; Pan, L. K.; Zhao, Q. F.; Sun, Z. *Nanoscale* **2010**, *2*, 1229–1232.
(17) Yu, P.; Zhu, K.; Norman, A. G.; Ferrere, S.; Frank, A. J.; Nozik, A. J. *J. Phys. Chem. B* **2006**, *110*, 25451–25454.
(18) Banerjee, S.; Mohapatra, S. K.; Das, P. P.; Misra, M. *Chem. Mater.* **2008**, *20*, 6784–6791.
(19) Shalom, M.; Albero, J.; Tachan, Z.; Martínez-Ferrero, E.; Zaban, A.; Palomares, E. *J. Phys. Chem. Lett.* **2010**, *1*, 1134–1138.
(20) Sero, I. M.; Bisquert, J. *J. Phys. Chem. Lett.* **2010**, *1*, 3046–3052.
(21) Zhu, G.; Lv, T.; Pan, L. K.; Sun, Z.; Sun, C. Q. *J. Alloys Compd.* **2011**, *509*, 362–365.
(22) Liu, L. P.; Hensel, J.; Fitzmorris, R. C.; Li, Y. D.; Zhang, J. Z. *J. Phys. Chem. Lett.* **2010**, *1*, 155–160.
(23) Martinez-Ferrero, E.; Sero, I. M.; Albero, J.; Gimenez, S.; Bisquert, J.; Palomares, E. *Phys. Chem. Chem. Phys.* **2010**, *12*, 2819–2821.
(24) Fan, S. Q.; Kim, D.; Kim, J. J.; Jung, D. W.; Kang, S. O.; Ko, J. *Electrochem. Commun.* **2009**, *11*, 1337–1339.
(25) Mora-Sero, I.; Gimenez, S.; Fabregat-Santiago, F.; Gomez, R.; Shen, Q.; Toyoda, T.; Bisquert, J. *Acc. Chem. Res.* **2009**, *42*, 1848–1857.
(26) Barea, E. M.; Shalom, M.; Gimenez, S.; Hod, I.; Mora-Sero, I.; Zaban, A.; Bisquert, J. *J. Am. Chem. Soc.* **2010**, *132*, 6834–6839.
(27) Zhu, G.; Xu, T.; Lv, T.; Pan, L. K.; Zhao, Q. F.; Sun, Z. *J. Electroanal. Chem.* **2011**, *650*, 248–251.
(28) Zhang, Q. X.; Zhang, Y. D.; Huang, S. Q.; Huang, X. M.; Luo, Y. H.; Meng, Q. B.; Li, D. M. *Electrochem. Commun.* **2010**, *12*, 327–330.
(29) Robel, I.; Subramanian, V.; Kuno, M.; Kamat, P. V. *J. Am. Chem. Soc.* **2006**, *128*, 2385–2393.
(30) Mora-Sero, I.; Gimenez, S.; Moehl, T.; Fabregat-Santiago, F.; Lana-Villareal, T.; Gomez, R.; Bisquert, J. *Nanotechnology* **2008**, *19*, 424007.
(31) Zhu, G.; Su, F. F.; Lv, T.; Pan, L. K.; Sun, Z. *Nanoscale Res. Lett.* **2010**, *5*, 1749–1754.
(32) Guijarro, N.; Lana-Villarreal, T.; Mora-Sero, I.; Bisquert, J.; Gomez, R. *J. Phys. Chem C* **2009**, *113*, 4208–4214.
(33) Sun, W. T.; Yu, Y.; Pan, H. Y.; Gao, X. F.; Chen, Q.; Peng, L. M. *J. Am. Chem. Soc.* **2008**, *130*, 1124–1125.
(34) Lee, H. J.; Yum, J. H.; Leventis, H. C.; Zakeeruddin, S. M.; Haque, S. A.; Chen, P.; Seok, S. I.; Grätzel, M.; Nazeeruddin, M. K. *J. Phys. Chem. C* **2008**, *112*, 11600–11608.
(35) Jin-nouchi, Y.; Naya, S.; Tada, H. *J. Phys. Chem. C* **2010**, *114*, 16837–16842.
(36) Guijarro, N.; Lana-Villarreal, T.; Shen, Q.; Toyoda, T.; Gomez, R. *J. Phys. Chem. C* **2010**, *114*, 21928–21937.
(37) Lin, S. C.; Lee, Y. L.; Chang, C. H.; Shen, Y. J.; Yang, Y. M. *Appl. Phys. Lett.* **2007**, *90*, 143517.
(38) Wang, G. M.; Yang, X. Y.; Qian, F.; Li, Yat; Zhang, J. Z. *Nano Lett.* **2010**, *10*, 1088–1092.
(39) Li, M.; Liu, Y.; Wang, H.; Shen, H.; Zhao, W. X.; Huang, H.; Liang, C. L. *J. Appl. Phys.* **2010**, *108*, 094304.
(40) Chen, J.; Wu, J.; Lei, W.; Song, J. L.; Deng, W. Q.; Sun, X. W. *Appl. Surf. Sci.* **2010**, *256*, 7438–7441.
(41) Lee, Y. L.; Huang, B. M.; Chien, H. T. *Chem. Mater.* **2008**, *20*, 6903–6905.
(42) Niitsoo, O.; Sarkar, S. K.; Pejoux, C.; Räuhle, S.; Cahen, D.; Hodes, G. *J. Photochem. Photobiol. A* **2006**, *181*, 306–313.

(43) Gao, X. F.; Sun, W. T.; Ai, G.; Peng, L. M. *Appl. Phys. Lett.* **2010**, *96*, 53104.
(44) Yang, Z.; Chen, C. Y.; Liu, C. W.; Chang, H. T. *Chem. Commun.* **2010**, *46*, 5485–5487.
(45) Chi, C. F.; Cho, H. W.; Teng, H.; Chuang, C. Y.; Chang, Y. M.; Hsu, Y. J.; Lee, L. *Appl. Phys. Lett.* **2011**, *98*, 012101.
(46) Lee, H. J.; Bang, J.; Park, J.; Kim, S. J.; Park, S. M. *Chem. Mater.* **2010**, *22*, 5636–5643.
(47) Zhang, Q. X.; Guo, X. Z.; Huang, X. M.; Huang, S. Q.; Li, D. M.; Luo, Y. H.; Shen, Q.; Toyoda, T.; Meng, Q. B. *Phys. Chem. Chem. Phys.* **2011**, *13*, 4659–4667.
(48) Gerbec, J. A.; Magana, D.; Washington, A.; Strouse, G. F. *J. Am. Chem. Soc.* **2005**, *127*, 15791–15800.
(49) Murugan, A. V.; Muraliganth, T.; Manthiram, A. *J. Phys. Chem. C* **2008**, *112*, 14665–14671.
(50) Panda, A. B.; Glaspell, G.; El-Shall, M. S. *J. Am. Chem. Soc.* **2006**, *128*, 2790–2791.
(51) Karan, S.; Mallik, B. *J. Phys. Chem. C* **2007**, *111*, 16734–16741.
(52) Wang, Q. B.; Seo, D. K. *Chem. Mater.* **2006**, *18*, 5764–5767.
(53) Qian, H. F.; Li, L.; Ren, J. C. *Mater. Res. Bull.* **2005**, *40*, 1726–1736.
(54) Zhu, G.; Pan, L. K.; Xu, T.; Sun, Z. *ACS Appl. Mater. Interfaces* **2011**, *3*, 1472–1478.
(55) Zhu, G.; Pan, L. K.; Xu, T.; Zhao, Q. F.; Lu, B.; Sun, Z. *Nanoscale* **2011**, *3*, 2188–2193.
(56) Ito, S.; Chen, P.; Comte, P.; Nazeeruddin, M. K.; Liska, P.; Pechy, P.; Grätzel, M. *Prog. Photovoltaics* **2007**, *15*, 603–612.
(57) Pedro, V. G.; Xu, X. Q.; Mora-Sero, I.; Bisquert, J. *ACS Nano* **2010**, *4*, 5783–5790.
(58) Lee, Y. L.; Chang, C. H. *J. Power Sources* **2008**, *185*, 584–588.
(59) Woodhousea, M.; Parkinson, B. A. *Chem. Soc. Rev.* **2009**, *38*, 197–210.
(60) Caramori, S.; Cristino, V.; Argazzi, R.; Meda, L.; Bignozzi, C. A. *Inorg. Chem.* **2010**, *49*, 3320–3328.
(61) Hiie, J.; Dedova, T.; Valdna, V.; Muska, K. *Thin Solid Films* **2006**, *511−512*, 443–447.
(62) Pan, L. K.; Sun, C. Q. *J. Appl. Phys.* **2004**, *95*, 3819–3821.
(63) Liu, Z. F.; Li, Y. J.; Zhao, Z. G.; Cui, Y.; Hara, K.; Miyauchi, M. *J. Mater. Chem.* **2010**, *20*, 492–497.
(64) Lee, K. M.; Suryanarayanan, V.; Ho, K. C. *Solar Energy Mater. Solar Cells* **2006**, *90*, 2398–2404.
(65) Chakrapani, V.; Baker, D.; Kamat, P. V. *J. Am. Chem. Soc.* **2011**, *133*, 9607–9615.
(66) Hossain, Md. A.; Jennings, J. R.; Koh, Z. Y.; Wang, Q. *ACS Nano* **2011**, *5*, 3172–3181.
(67) Hossain, Md. A.; Yang, G. W.; Parameswaran, M.; Jennings, J. R.; Koh, Z. Y.; Wang, Q. *J. Phys. Chem. C* **2010**, *114*, 21787–21884.
(68) Kundu, S.; Lee, H.; Liang, H. *Inorg. Chem.* **2009**, *48*, 121–128.
(69) Tu, W.; Liu, H. *Chem. Mater.* **2000**, *12*, 564–567.
(70) Sun, C. Q.; Sun, Y.; Ni, Y.; Zhan, X.; Pan, J.; Wang, X. H.; Zhou, J.; Li, L. T.; Zheng, W.; Yu, S.; Pan, L. K.; Sun, Z. *J. Phys. Chem. C* **2009**, *113*, 20009–20019.
(71) Chang, C. H.; Lee, Y. L. *Appl. Phys. Lett.* **2007**, *91*, 053503.
(72) Komarneni, S.; Li, D.; Newalkar, B.; Katsuki, H.; Bhalla, A. S. *Langmuir* **2002**, *18*, 5959–5962.
(73) Chen, D.; Shen, G.; Tang, K.; Lei, S.; Zheng, H.; Qian, Y. *J. Cryst. Growth* **2004**, *260*, 469–474.
(74) Zhang, H.; Wang, L.; Xiong, H.; Hu, L.; Yang, B.; Li, W. *Adv. Mater.* **2003**, *15*, 1712–1715.
(75) Li, L.; Qian, H.; Ren, J. *Chem. Commun.* **2005**, 528–530.
(76) Shanmugam, M.; Baroughi, M. F.; Galipeau, D. *Thin Solid Films* **2010**, *518*, 2678–2682.
(77) Diguna, L. J.; Shen, Q.; Kobayashi, J.; Toyada, T. *Appl. Phys. Lett.* **2007**, *91*, 023116.